Electronic Supplementary Material (ESI) for RSC Advances
This journal is © The Royal Society of Chemistry 2016

Electronic Supplementary Information

Grafting of multi-sensitive PDMAEMA brushes onto carbon nanotubes by ATNRC: tunable thickening/thinning and self-assembly behaviors in aqueous solutions

Yeqiang Tan,‡ Wenqian Zhang,‡ Yanhui Li, Yanzhi Xia*, and Kunyan Sui*

Collaborative Innovation Center for Marine Biomass Fibers, Materials and Textiles of Shandong Province, School of Materials Science and Engineering, Qingdao University, Qingdao, 266071, China. E-mail: kunyansui@163.com.

Table S1 Constituent parameters of MWNTs-*g*-PDMAEMA.

Sample	Feed ratio [a]	M_n [b]	M_w/M_n [b]	f (wt.%) [c]	Graft density [d]
MWNTs-*g*-PDMAWMA$_{50}$	50:1	4770	1.05	75.4	1/129
MWNTs-*g*-PDMAWMA$_{100}$	100:1	8420	1.17	67.2	1/342
MWNTs-*g*-PDMAWMA$_{150}$	150:1	11170	1.07	37.4	1/1558

[a] The ratio of molar weight of DMAEMA monomer to EBiB.
[b] The molecular weight data of PDMAEMA determined by GPC.
[c] The weight fraction of PDMAEMA in MWNTs-*g*-PDMAEMA calculated from TGA.
[d] The average graft density (C/PDMAEMA chain) calculated from GPC and TGA.

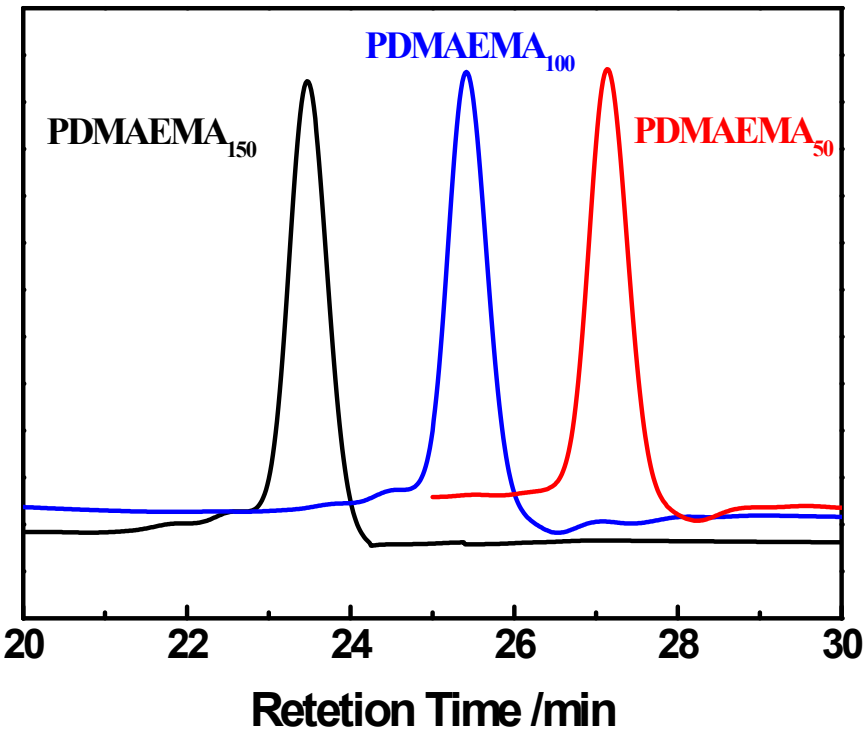

Fig. S1 GPC traces of PDMAEMA. The single peaks of typical Gaussian distributions indicated formation of desired PDMAEMA homopolymer. The number-average molecular weight is 4770, 8420, 11170, and PDI (M_w/M_n) is 1.05, 1.17 and 1.07, respectively, clarifying that the ATRP polymerization of PDMAEMA were well-controlled.

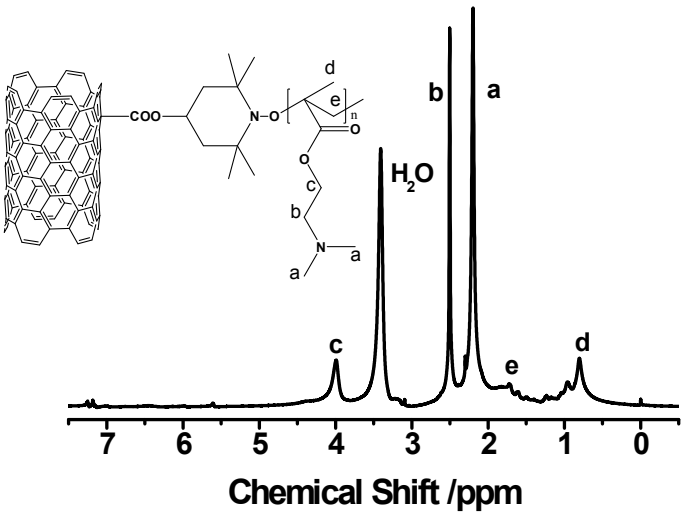

Fig. S2 ^{1}H NMR spectra of MWNTs-*g*-PDMAEMA$_{100}$ in D_2O.

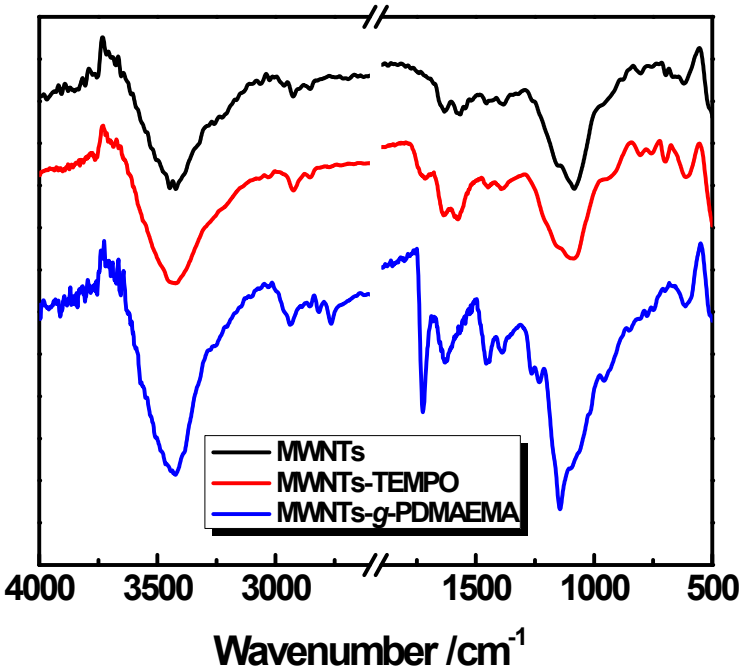

Fig. S3 FT-IR spectrum of MWNTs, MWNTs-COOH and MWNTs-g-PDMAEMA. In MWNTs-TEMPO clearly showed that the characteristic carboxyl group stretching vibrations appeared at 1700 cm^{-1}. The appearance of characteristic absorption bands at 2950 cm^{-1} (C-H stretching of methyl and $-CH_2-$ groups), 2821 and 2770 cm^{-1} (C-H stretching of $N-(CH_3)_2$ group), 1726 cm^{-1} (C=O stretching), 1454 cm^{-1} ($-CH_2-$ bending(scissors) vibration and CH_3 antisymmetric deformation), and 1150 cm^{-1} (C-C-N bending) demonstrated the presence of PDMAEMA chains on MWNTs-g-PDMAEMA.

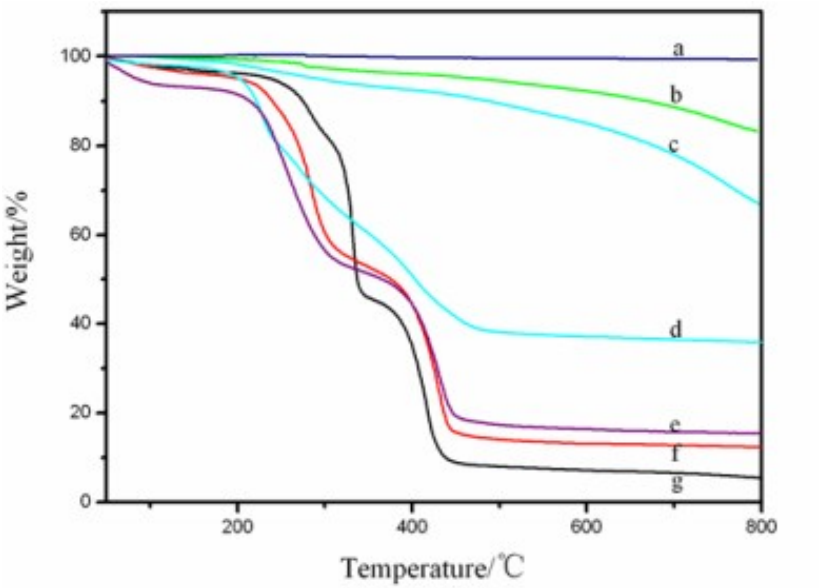

Fig. S4 TGA curves of pristine MWNTs (a), MWNTs-COOH (b), MWNTs-TEMPO (c), MWNTs-g-PDMAEMA150 (d), MWNTs-g-PDMAEMA100 (e), MWNTs-g-PDMAEMA50 (f), and PDMAEMA (g) powders.

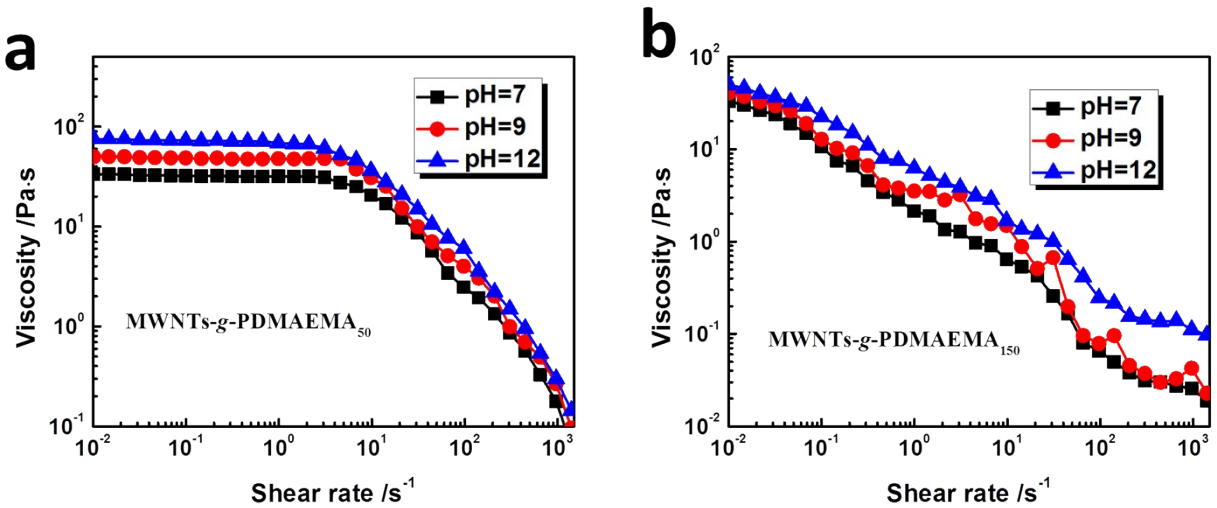

Fig. S5 η as a function of $\dot{\gamma}$ for MWNTs-g-PDMAEMA$_{50}$ (a) MWNTs-g-PDMAEMA$_{150}$ (b) suspensions with different pH at 25 ˚C (C = 20 wt%).

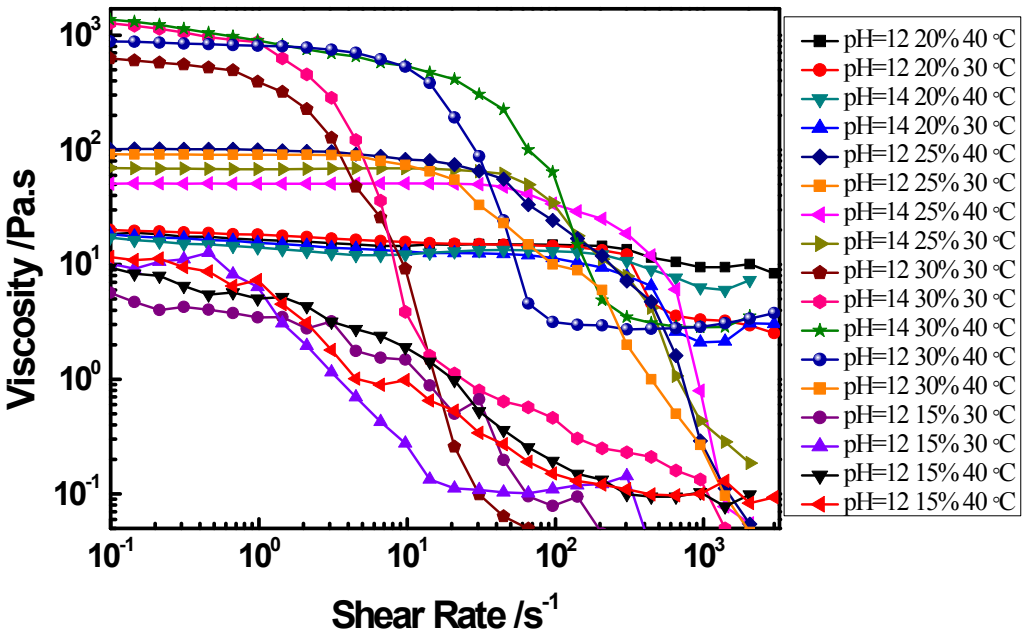

Fig S6. η as a function of $\dot{\gamma}$ for MWNTs-*g*-PDMAEMA$_{100}$ suspensions at various pH values, tempratures and concentration. It is obvious that no shear-thickening behavior take placed at all pH, temperatures and concentrations.

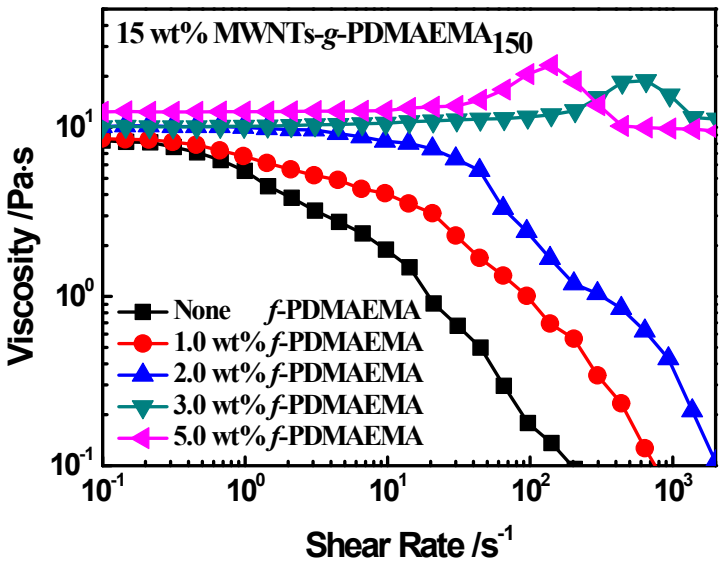

Fig. S7 η as a function of $\dot{\gamma}$ for MWNT-g-PDMAEMA$_{150}$/*f*-PDMAEMA suspension with different concentration of *f*-PDMAEMAM at pH=14.

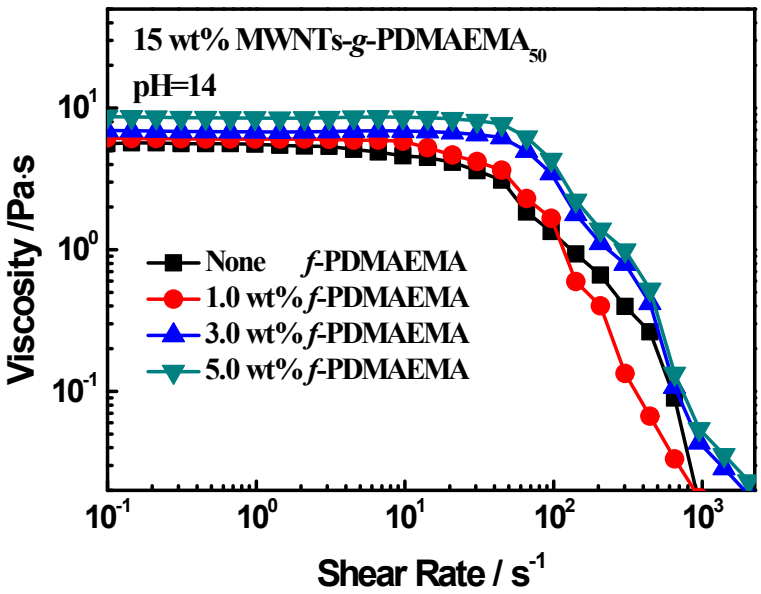

Fig. S8 η as a function of $\dot{\gamma}$ for MWNT-g-PDMAEMA$_{50}$/*f*-PDMAEMA suspension with different concentration of *f*-PDMAEMAM at pH=14.

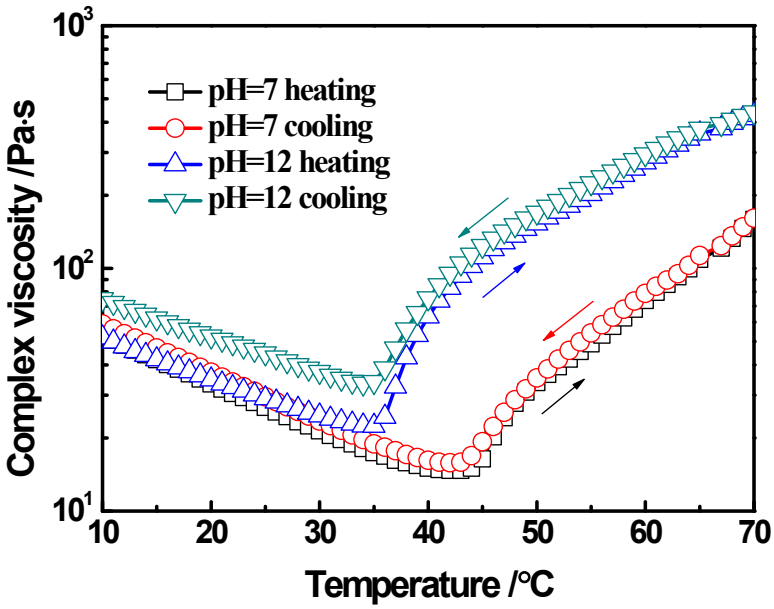

Fig. S9 Temperature dependence of complex viscosity for MWNTs-*g*-PDMAEMA$_{100}$ aqueous solution at pH 7 and 12.

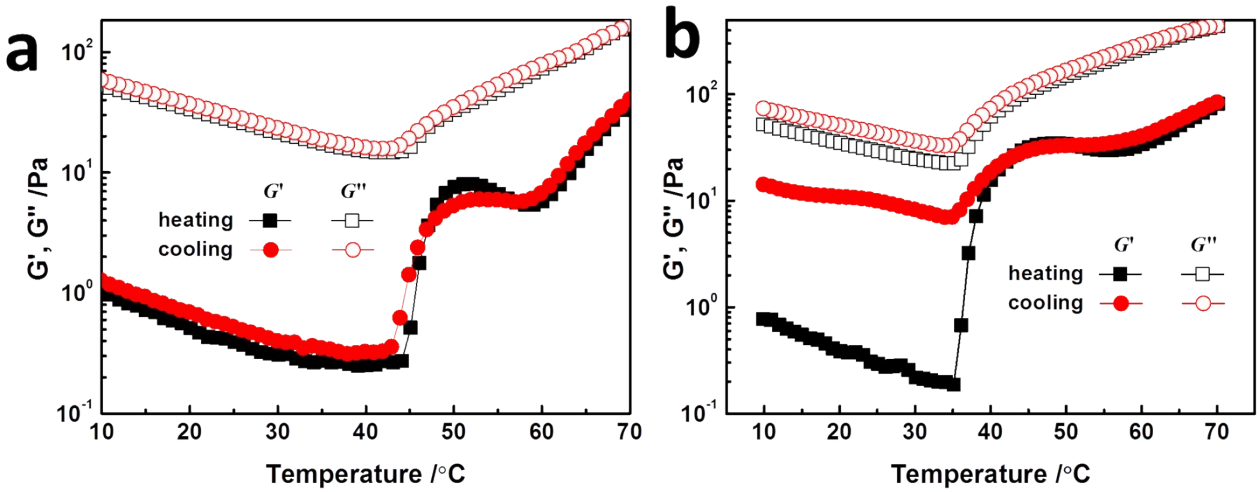

Fig. S10 Dynamic temperature ramp for MWNTs-*g*-PDMAEMA100 suspension (C = 20 wt%) at pH=7 (a) and 12 (b) monitored at 1 rad s^{-1} with a temperature rate of 1 °C min^{-1}.